Grazing incidence fast atom diffraction in high-pressure conditions

A. Mukherjee, A. Momeni, A.R. Allouche, E.M. Staicu Casagrande, T. Minea, H. Khemliche

Grazing Incidence Fast Atom Diffraction in high-pressure conditions

A. Mukherjee[1], A. Momeni[1,2], A. R. Allouche[1,3], E.M. Staicu Casagrande[1], T. Minea[4], H. Khemliche[1]*

[1]*Université Paris Saclay, CNRS, Institut des Sciences Moléculaires d'Orsay, 91405 Orsay, France*

[2]*CY Cergy Paris Université, 95000 Cergy, France*

[3]*Laboratoire de Physique et Modélisation (LPM), EDST, Lebanese University, 1300 Tripoli, Lebanon*

[4]*Université Paris-Saclay, CNRS, Laboratoire de Physique des Gaz et des Plasmas, 91405 Orsay, France*

[*]*Corresponding author: hocine.khemliche@universite-paris-saclay.fr*

Abstract

Grazing Incidence Fast Atom Diffraction (GIFAD) is a recent technique for characterizing surface structures and real-time monitoring of thin film growth. Up to now, GIFAD has only been used in Ultra-High-Vacuum conditions, typically in the range of 10^{-10} to 10^{-8} mbar, and has therefore only been considered for high vacuum deposition methods like Molecular Beam Epitaxy or very low-pressure Chemical Vapor Deposition (CVD). At pressures exceeding 10^{-6} mbar, gas phase collisions along the atom beam trajectory not only reduce the mean free path but also degrade the beam coherence length and thus potentially suppress the diffraction signal. In addition, pressures lower than 10^{-5} mbar are required to maintain a low noise level on the scattered particle detector. In a new configuration, we demonstrate that GIFAD can operate at pressure as high as 10^{-2} mbar of argon with well-contrasted diffraction patterns. This opens wide avenues for the study of surface reactivity, thin film growth in Magnetron Sputtering Deposition, where electron diffraction is inevitably perturbed by the electromagnetic fields. This High-Pressure version of GIFAD could also be extended to Reactive Pulsed Laser Deposition and many CVD variants.

Keywords: Surface structure analysis, Grazing Incidence Fast Atom Diffraction, Thin film growth, Atom-surface interactions, Decoherence.

1. Introduction

Atom beam diffraction at thermal energies has been used in many branches of surface science for decades to study atom surface interactions, surface structure, nucleation and growth of thin films [1]. Despite its many advantages, this diffraction regime has seldom been used for real-time analysis due to its slowness since the detection of the scattered atoms is performed point by point in space [2]. Grazing Incidence Fast Atom Diffraction (GIFAD), the high-energy counterpart, has developed as an effective and complementary method for both surface analysis and thin film growth monitoring. Due to the grazing trajectory of energetic atoms, the parallel and perpendicular motions can be decoupled when considering a flat surface, and the diffraction process can be understood by considering only the slow motion, normal to the surface, which is then similar to the incidence of thermal energy atoms. For both thermal and fast atoms, the diffraction patterns essentially provide information about the Potential Energy Surface (PES) [3–5]. However, the grazing incidence geometry in GIFAD strongly reduces decoherence due to thermal vibrations of the surface atoms [6], therefore much higher normal energies can be achieved. In most situations, the normal energy is much larger than the potential well, which is typically 5-15 meV for He atoms [7,8], the weak attractive contribution to the PES can then be neglected, so the PES can be considered equivalent to the intrinsic electron density profile of the surface [9].

The de Broglie wavelength of an atom with mass m and a velocity v is $\lambda_{dB} = h / mv$. For He atoms with 1 keV energy $\lambda_{dB} = 0.45$ pm. To observe diffraction, the transverse coherence width (i.e. width of the associated wave packet) $L_c \approx \lambda_{dB} / \theta$ [10] where θ is the beam divergence angle, needs to be larger than twice the projected crystal period (d) as depicted in Fig. 1.

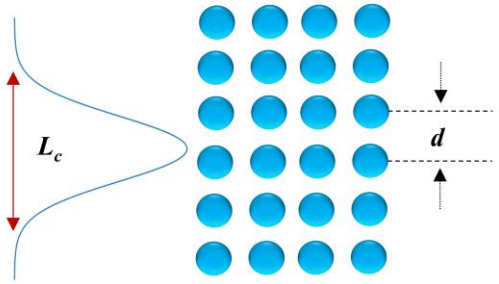

***Fig. 1**. Schematic of the diffraction condition of a wave packet of width L_c interacting with a surface.*

This condition imposes a stringent limit on the beam divergence, with a typical value below 1 mrad. For comparison, the angle between two consecutive diffraction orders (Bragg angle) for 1 keV He atoms falls in the range of 1 to 2 mrad for most inorganic materials.

GIFAD was first observed on insulator surfaces [11,12] and subsequently on metals [13,14] and semiconductors [8,15]. With He atoms as a probe, GIFAD has also shown an effectiveness in

providing detailed real-time information on the growth and organization dynamics of semiconductors [16] and ultrathin organic films [17] thanks to its non-destructive character.

All previous studies were performed in Ultra High Vacuum (UHV) conditions. However, most methods for growing thin films operate at pressures well beyond 10^{-6} mbar. Among these, Magnetron Sputter Deposition (MSD) typically operates between 10^{-3} and 10^{-2} mbar [18]; reactive Pulsed Laser deposition operates up to 0.1 mbar [19], and CVD pressures span from UHV to the atmosphere [20,21].

Possible operation of GIFAD at higher pressures raises the central question regarding the subsequent coherence length. Elastic collisions eventually produce broadening of the beam that, as described above, could be detrimental to observation of diffraction.

This paper demonstrates that the beam coherence can be preserved by the careful design of a double differential pumping system. Well-resolved diffraction patterns from LiF (001) can be observed at argon pressures up to 10^{-2} mbar.

2. Methods

A schematic of the scattering chamber is shown in Fig.2. The production, collimation and detection of the neutral He beam is similar to that described in previous publications, e.g. [4]. The He^0 beam was produced by neutralizing a He^+ beam in a gas cell and further collimated by two apertures, the first one with size 400×60 µm and the second one with a diameter of 150 µm. The scattered atoms are collected on a detector composed of microchannel plates and a phosphor screen; the diffraction images are further captured by a CCD camera located on the air side.

The major evolution is the differential pumping configuration. Here the second beam collimation aperture (150 µm) also serves to reduce the gas leakage between the atom gun and the scattering chamber. To reduce the noise level on the detector, the pressure in the detection volume must remain in the 10^{-6} mbar range, despite the 10^{-2} mbar in the scattering chamber. Therefore, the challenge was to find an effective compromise that considerably reduces the conductance between the scattering and detection volumes while collecting both the direct and scattered beams. We shall recall that collection of the direct beam is essential for an accurate determination of the normal energy and subsequently for the corresponding equipotential line of the PES. The solution consists in a series of four apertures, with dimensions from 4 to 10 mm, set close to the sample. In this configuration, the effective length of the high pressure region is reduced to $l_2 = 65$ mm $\cong 2l_1$ (Fig. 2). At an argon gas pressure $P = 10^{-2}$ mbar, the mean free path l_{MFP} of thermal He atoms is in the range of a cm. For fast He atoms, the cross section σ for elastic scattering on Ar has been measured from 40-850 eV [22], so l_{MFP} can be expressed as:

$$l_{MFP} = kT / P\sigma \quad (1)$$

From a rough extrapolation on the measured cross-sections to 1 keV, we set $\sigma \cong 4\times10^{-16}$ cm^2, which yields a mean free path of 10 cm at 10^{-2} mbar. Increasing l_2 would result in a strong beam attenuation; the chosen value is therefore a reasonable compromise that lets sufficient space for the sample holder.

The experiment is performed with a LiF(001) sample that is cleaved in air and immediately transferred to the UHV chamber on a five-axis manipulator. A clean surface is achieved by annealing around 300°C for a few hours. He atoms at 1 keV energy where scattered at an angle between 0.76° and 0.78° from the sample maintained at room temperature. Argon gas with 99.999% purity is introduced into the chamber using a leak valve; at the highest pressure used in the experiment (10^{-2} mbar), the mean signal/noise ratio on the detector remained at the acceptable value of ~25:1.

3. Results and Discussions

The experimental diffraction images measured at different pressures along the <100> and <110> directions are shown in Fig. 3a-d. The lowest pressures, 10^{-8} mbar and 5.6×10^{-9} mbar respectively, correspond to the base vacuum level. The diffraction spectra for the <100> direction, obtained by projecting the intensity contained in between the two Laue circles of polar radius 0.78°±0.05° (which corresponds to a normal energy of 185 meV±23 meV), are shown in Fig.3e. At first glance, the

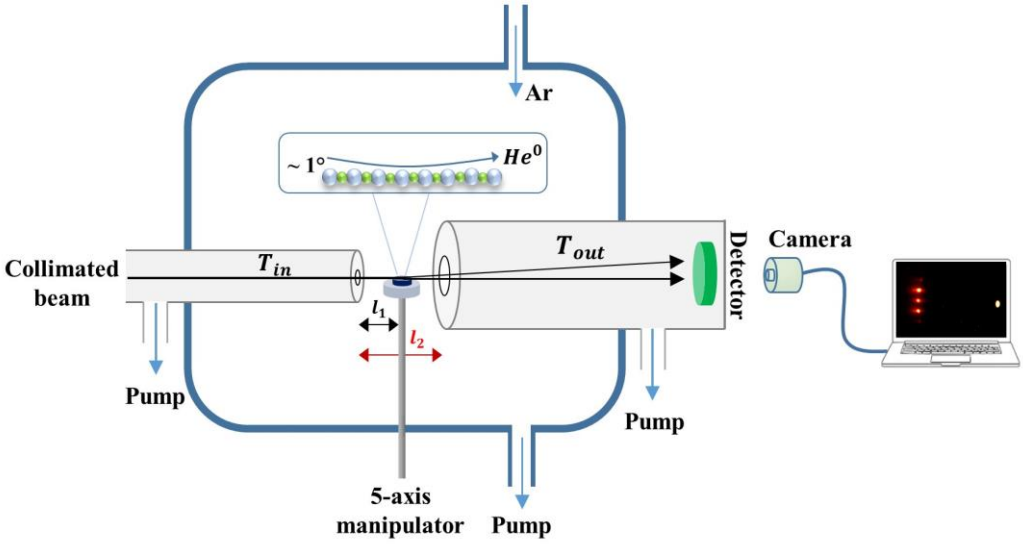

Fig. 2. *Schematic of high-pressure GIFAD setup. T_{in} and T_{out} are the entrance and exit tubes having diameters 150 µm and 4 mm respectively. The separation between T_{in} and T_{out} and T_{in} and sample are $l_2$and l_1 respectively. LiF(001) sample is shown in blue color. $l_2 = 2l_1 = 65$ mm.*

diffraction signal measured at 3.6×10^{-3} mbar shows an intensity loss by a factor of ~3.5 with respect to the signal measured at the base pressure.

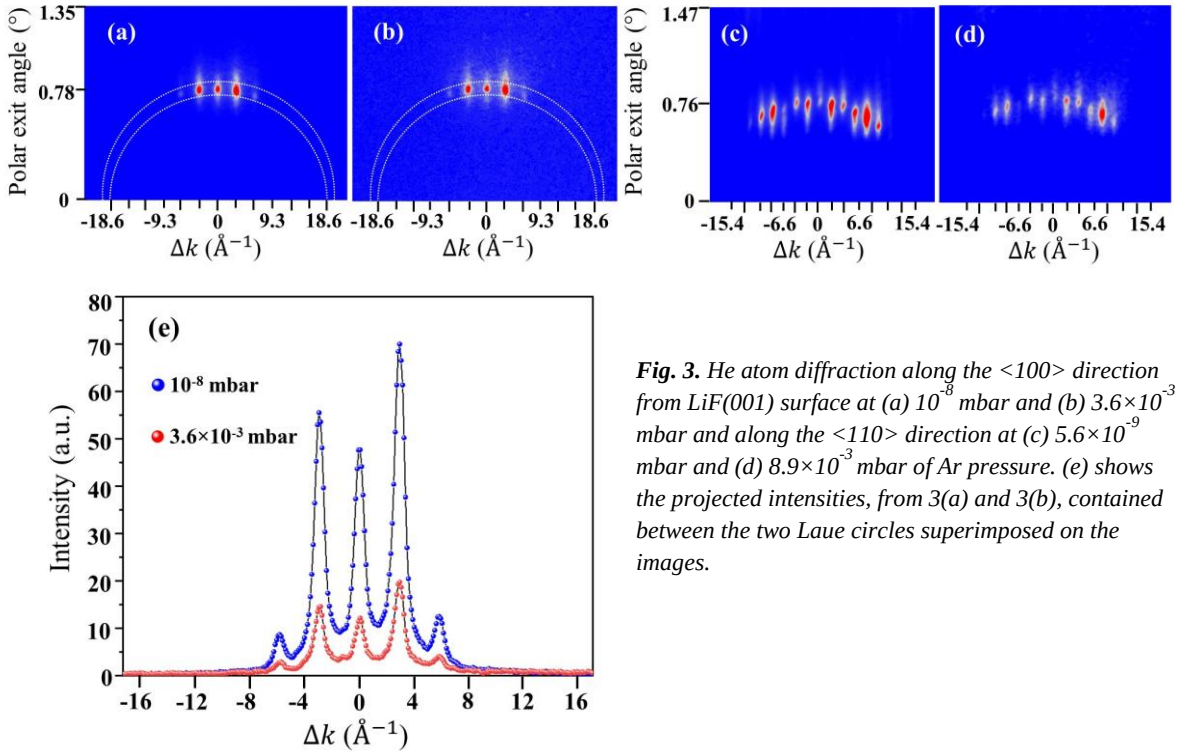

Fig. 3. *He atom diffraction along the <100> direction from LiF(001) surface at (a) 10^{-8} mbar and (b) 3.6×10^{-3} mbar and along the <110> direction at (c) 5.6×10^{-9} mbar and (d) 8.9×10^{-3} mbar of Ar pressure. (e) shows the projected intensities, from 3(a) and 3(b), contained between the two Laue circles superimposed on the images.*

It is worth comparing the pressure dependence of the attenuation factor for both the direct beam, where the sample is removed from the incident beam path, and for the scattered beam; these are shown respectively in Fig.4a and 4b. The intensity loss of the direct beam can only be related to the gas-phase collisions between He and Ar atoms. As expected, the direct beam follows a single exponential decay according to the Beer-Lambert [23] principle

$$I = I_0 \exp(-n\sigma l_2) \qquad (2)$$

where I_0 is the intensity measured without gas, n is the number density of the argon gas and l_2 is the path length traversed by the beam. We used a modified equation to fit the data as follows,

$$I = I_0 \exp(-p/p_s) \qquad (3)$$

Where $p_s = kT/\sigma l_2$; k and T are the Boltzmann constant and absolute temperature respectively. The parameter p_s can be obtained from fitting the experimental data, and one can then derive the scattering cross section. We find $p_s = 3.9\times10^{-3}$ mbar, leading to $\sigma = 1.5\times10^{-15}$ cm^2 assuming a fast pressure drop at the entrance and exit tubes apertures.

Contrary to the direct beam intensity, the decay of the scattered beam can no longer be fitted by a single exponential function as shown in Fig. 4b, but fits rather well with a bi-exponential curve (see the semi-log graph in the inset of Fig. 4b), indicating two regimes of scattering. A plausible explanation points to an additional scattering contribution from species (H_2O, CO_2, etc.) adsorbed on

the sample surface due to contamination of the injected gas. This explanation is confirmed by the fact that the scattered beam intensity does not fully recover when the pressure is brought back to its initial value. The decay parameters obtained from the bi-exponential fit yield p_{s1} = 4.2×10^{-3} mbar and p_{s2} =7.16×10^{-5} mbar. One can note that, $p_{s1} \cong p_s$ demonstrating that both direct and scattered beam experience similar scattering process from the surrounding argon gas.

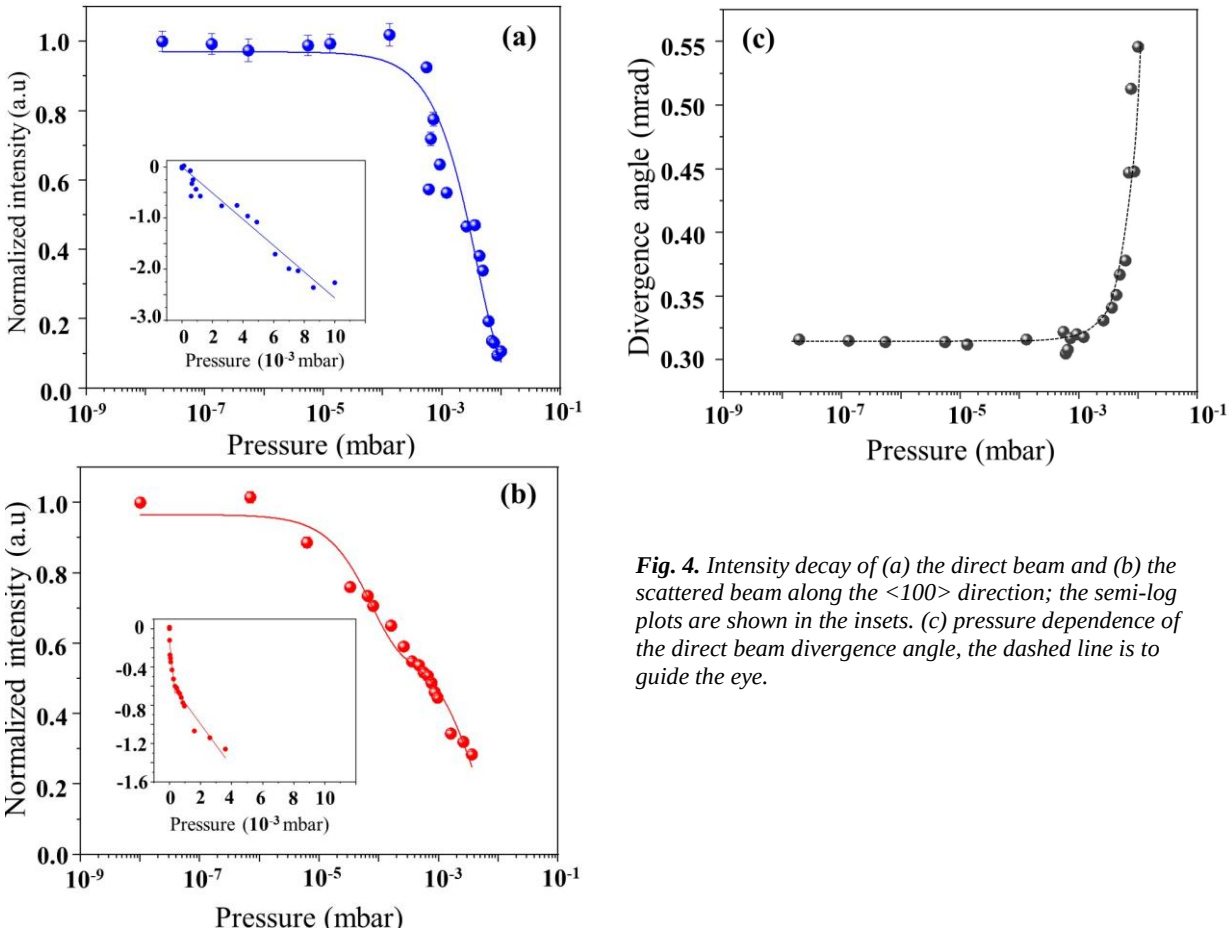

Fig. 4. *Intensity decay of (a) the direct beam and (b) the scattered beam along the <100> direction; the semi-log plots are shown in the insets. (c) pressure dependence of the direct beam divergence angle, the dashed line is to guide the eye.*

At the highest pressure investigated, 10^{-2} mbar, a clear diffraction pattern is still observed, indicating that the collision-induced broadening of the direct beam, along the path preceding the surface interaction (l_1), does not significantly reduce the transverse coherence length. The divergence angle of the direct beam along the full beam path l_2, shown in Fig. 4c, remains nearly constant up to ~5x10^{-4} mbar and then increases quasi-exponentially. The divergence angle is derived from the beam diameter at an intensity of $1/e^2$ of the peak amplitude. At 10^{-2} mbar pressure and based on the quasi-exponential behavior, the actual beam divergence at the sample position is that measured at 5×10^{-3} mbar, so only ~0.37 mrad as compared to the value of 0.32 mrad measured without the Ar gas. This weak degradation of the beam divergence explains the persistence of a well-contrasted diffraction pattern.

4. Conclusions and perspectives

We have demonstrated that grazing incidence diffraction of fast He atoms from a clean crystalline surface can be observed at surrounding argon gas pressures as high as 10^{-2} mbar. Notwithstanding the fact that, the direct beam intensity has lost 90% of its intensity at this pressure, and that the available differential cross-section for He scattering on Ar [24] drops by less than a factor of 3 in amplitude between zero and 0.05° scattering angles, the coherence width remains sufficient for preserving diffraction. Interestingly, calculations performed by Karlovets et al. [25] on the elastic scattering of an electron wavepacket on a hydrogen atom show a clear effect of the wave packet transverse size (i.e. transverse coherence width) of the differential cross-section; large angle contributions to the later decreases with increasing transverse coherence width. These results have been further confirmed by Sarkadi et al. [26] on the scattering of 75 keV protons on atomic hydrogen. Although a detailed analysis on the effect of beam coherence on the final beam divergence is well beyond the scope of this work, high beam collimation conditions seem to represent a protection against decoherence.

This new high-pressure GIFAD configuration, which we name HP-GIFAD, offers many opportunities for the study of surface reactivity and should also represents an alternative diffraction tool for monitoring thin film growth in high-pressure conditions. For surface structure characterization, the He probe has been selected for its inertness; this key property is also favorable in limiting gas phase interactions with the surroundings species.

Real-time monitoring during thin film growth has always been a challenge. Reflection High Energy Electron Diffraction (RHEED) showed powerful in monitoring film growth in Molecular Beam Epitaxy chambers [27,28]. In its high pressure version, RHEED has seen its use extended to other deposition modes, such as Pulsed Laser Deposition[29] or Atomic Layer Deposition[30]. In a layer-by-layer growth mode, RHEED provides a direct information of film thickness through oscillations of the reflected intensity[31]. Despite some complex attempts[32], application of RHEED in MSD suffers severe limitations because of the stray electromagnetic fields. HP-GIFAD may thus offer an alternative solution for accessing film growth properties (growth mode, crystalline structure, defect density). Due to the extreme GIFAD sensitivity to the surface defects, it should provide valuable insight into the influence of plasma parameters on the growing film. However, substrate contamination plays a pivotal role in thin film depositions, and the quality of the film is also affected. So, the UHV approach (leak-free system, baking, selection of materials, etc.) is the best solution to keep the substrate as well as the growing layer free from contamination, this scheme naturally implies the use of a high-purity process gas. The benefit might be decisive for the more challenging case of HiPIMS (High Power Impulse Magnetron Sputtering), a recent variant of MSD [33]. HiPIMS produces better films with greater density and crystallinity but its development is hindered the complexity related to the large number of adjustable parameters (pulse power, pulse duration, duty

cycle, argon gas pressure, oxygen pressure for reactive sputtering, substrate temperature, ion acceleration). We suggest that HP-GIFAD could be very effective in precisely controlling the growth process in HiPIMS.

Declaration of competing interest

The authors declare that they have no competing financial interests that could have appeared to influence the work reported in this paper.

CRediT authorship contribution statement

A. Mukherjee: Investigation, Analysis, Writing-original draft, *A. Momeni*- Participate in experiments, review, and editing, *A. R. Allouche*- Participate in experiments, review and editing, *E. M. Staicu Casagrande*- Participate in experiments, *T. Minea*- Supervision, Resources, review and editing, *H. Khemliche*- Conceptualization, Supervision, Resources, Project administration, Data curation, review and editing.

Data availability

No data was used for the research described in this article.

Acknowledgments

This work has been partially funded by 'Investissements d´Avenir', LabEx PALM (ANR-10-LABX-0039-PALM).

We are grateful to Hynd Remita from the Institut de Chimie Physique (LCP, UMR 8000) for the irradiation of the LiF samples.

We also acknowledge Sylvain Lupone for his technical assistance.

References

[1] D. Farías and K.-H. Rieder. Atomic beam diffraction from solid surfaces. Rep. Prog. Phys. 61 (1998) 1575-1664. https://doi.org/10.1088/0034-4885/61/12/001.

[2] M. J. Cardillo, C. S. Y. Ching, E. F. Greene, and G. E. Becker, Molecular-beam apparatus for the study of gas–surface interactions, Journal of Vacuum Science and Technology 15 (1978) 423-

428.https://doi.org/10.1116/1.569586.

[3] H. Winter, A. Schüller, J. Seifert, J. Lienemann, S. Wethekam, M. Busch, Fast atom diffraction at surfaces, Journal of Physics: Conference Series. 388 (2012) 012047. https://doi.org/10.1088/1742-6596/388/1/012047.

[4] G.A. Bocan, H. Breiss, S. Szilasi, A. Momeni, E.M.S. Casagrande, M.S. Gravielle, E.A. Sánchez, H. Khemliche, Anomalous KCl(001) Surface Corrugation from Fast He Diffraction at Very Grazing Incidence, Physical Review Letters. 125 (2020) 96101. https://doi.org/10.1103/PhysRevLett.125.096101.

[5] G.A. Bocan, M.S. Gravielle, GIFAD for He/KCl(001). Structure in the pattern for <110> incidence as a measure of the projectile-cation interaction, Nuclear Instruments and Methods in Physics Research, Section B: Beam Interactions with Materials and Atoms. 421 (2018) 1–6. https://doi.org/10.1016/j.nimb.2018.02.004.

[6] P. Rousseau, H. Khemliche, N. Bundaleski, P. Soulisse, A. Momeni, P. Roncin, Surface analysis with grazing incidence fast atom diffraction (GIFAD), Journal of Physics: Conference Series. 133 (2008) 012013. https://doi.org/10.1088/1742-6596/133/1/012013.

[7] G.A. Bocan, H. Breiss, S. Szilasi, A. Momeni, E.M. Staicu Casagrande, E.A. Sánchez, M.S. Gravielle, H. Khemliche, Dynamical effects as a window into van der Waals interactions in grazing-incidence fast He-atom diffraction from KCl(001), Physical Review B. 104 (2021) 235401. https://doi.org/10.1103/PhysRevB.104.235401.

[8] M. Debiossac, A. Zugarramurdi, H. Khemliche, P. Roncin, A.G. Borisov, A. Momeni, P. Atkinson, M. Eddrief, F. Finocchi, V.H. Etgens, Combined experimental and theoretical study of fast atom diffraction on the β2(2×4) reconstructed GaAs(001) surface, Physical Review B - Condensed Matter and Materials Physics. 90 (2014) 1–13. https://doi.org/10.1103/PhysRevB.90.155308.

[9] N. Esbjerg, J.K. Nørskov, Dependence of the He-Scattering Potential at Surfaces on the Surface-Electron-Density Profile, Physical Review Letters. 45 (1980) 807–810. https://doi.org/10.1103/PhysRevLett.45.807.

[10] D.R. Frankl, Comments on "Coherence legth and/or Transfer width?", Surface Science Letters. 84 (1979) L485-L488.

[11] P. Rousseau, H. Khemliche, A.G. Borisov, P. Roncin, Quantum Scattering of Fast Atoms and Molecules on Surfaces, Physical Review Letters. 98 (2007) 016104. https://doi.org/10.1103/PhysRevLett.98.016104.

[12] A. Schüller, S. Wethekam, H. Winter, Diffraction of Fast Atomic Projectiles during Grazing Scattering from a LiF(001) Surface, Physical Review Letters. 98 (2007) 016103. https://doi.org/10.1103/PhysRevLett.98.016103.

[13] N. Bundaleski, H. Khemliche, P. Soulisse, P. Roncin, Grazing incidence diffraction of keV helium atoms on a Ag(110) surface, Physical Review Letters. 101 (2008) 177601. https://doi.org/10.1103/PhysRevLett.101.177601.

[14] M. Busch, A. Schüller, S. Wethekam, H. Winter, Fast atom diffraction at metal surface, Surface Science. 603 (2009) L23–L26. https://doi.org/10.1016/j.susc.2008.12.021.

[15] H. Khemliche, P. Rousseau, P. Roncin, V.H. Etgens, F. Finocchi, Grazing incidence fast atom

diffraction: An innovative approach to surface structure analysis, Applied Physics Letters. 95 (2009) 151901. https://doi.org/10.1063/1.3246162.

[16] P. Atkinson, M. Eddrief, V.H. Etgens, H. Khemliche, M. Debiossac, A. Momeni, M. Mulier, B. Lalmi, P. Roncin, Dynamic grazing incidence fast atom diffraction during molecular beam epitaxial growth of GaAs, Applied Physics Letters. 105 (2014) 021602. https://doi.org/10.1063/1.4890121.

[17] A. Momeni, E.M. Staicu Casagrande, A. Dechaux, H. Khemliche, Ultrafast Crystallization Dynamics at an Organic-Inorganic Interface Revealed in Real Time by Grazing Incidence Fast Atom Diffraction, Journal of Physical Chemistry Letters. 9 (2018) 908–913. https://doi.org/10.1021/acs.jpclett.7b03246.

[18] J.T. Gudmundsson, Physics and technology of magnetron sputtering discharges, Plasma Sources Science and Technology. 29 (2020) 113001. https://doi.org/10.1088/1361-6595/abb7bd.

[19] P. Bílková, B. Mitu, V. Marotta, G. Mattei, S. Orlando, A. Santagata, Reactive pulsed laser deposition of zinc oxide thin films, Applied Physics A: Materials Science and Processing. 79 (2004) 1061–1065. https://doi.org/10.1007/s00339-004-2629-7.

[20] H. Sun, C. Wang, S. Pang, X. Li, Y. Tao, H. Tang, M. Liu, Photocatalytic TiO2 films prepared by chemical vapor deposition at atmosphere pressure, Journal of Non-Crystalline Solids. 354 (2008) 1440–1443. https://doi.org/10.1016/j.jnoncrysol.2007.01.108.

[21] N.S. Mueller, A.J. Morfa, D. Abou-Ras, V. Oddone, T. Ciuk, M. Giersig, Growing graphene on polycrystalline copper foils by ultra-high vacuum chemical vapor deposition, Carbon. 78 (2014) 347–355. https://doi.org/10.1016/j.carbon.2014.07.011.

[22] D.N. Ruzic, S.A. Cohen, Total scattering cross sections and interatomic potentials for neutral hydrogen and helium on some noble gases, The Journal of Chemical Physics. 83 (1985) 5527–5530. https://doi.org/10.1063/1.449674.

[23] P. Dehmer, L. Wharton, Absolute total scattering cross sections for ^{7}Li on He, Ne, Kr, and Xe, The Journal of Chemical Physics. 57 (1972) 4821–4835. https://doi.org/10.1063/1.1678154.

[24] R. S. Gao, L. K. Johnson, D. E. Nitz, K. A. Smith, and R. F. Stebbings, Absolute differential cross sections for small-angle elastic scattering in helium —rare-gas collisions at kev energies, Physical Review A. 36 (1987) 3077-3082. https://doi.org/10.1103/PhysRevA.36.3077

[25] D. V. Karlovets, G.L. Kotkin, V.G. Serbo, Scattering of wave packets on atoms in the Born approximation, Physical Review A - Atomic, Molecular, and Optical Physics. 92 (2015) 052703. https://doi.org/10.1103/PhysRevA.92.052703.

[26] L. Sarkadi, I. Fabre, F. Navarrete, R.O. Barrachina, Loss of wave-packet coherence in ion-atom collisions, Physical Review A. 93 (2016) 032702. https://doi.org/10.1103/PhysRevA.93.032702.

[27] W.P. Mccray, MBE deserves a place in the history books, Nature Nanotechnology. 2 (2007) 259–261. https://doi.org/10.1038/nnano.2007.121.

[28] W. Braun, Applied RHEED: Reflection High-Energy Electron Diffraction during crystal growth, 1st Edition, Springer, Berlin, 1999.

[29] D.H.A. Blank, G.J.H.M. Rijnders, G. Koster, H. Rogalla, In-situ monitoring by reflective high energy electron diffraction during pulsed laser deposition, Applied Surface Science. 138–139 (1999) 17–23. https://doi.org/10.1016/S0169-4332(98)00470-X.

[30] R. Bankras, J. Holleman, J. Schmitz, M. Sturm, A. Zinine, H. Wormeester, B. Poelsema, In situ reflective high-energy electron diffraction analysis during the initial stage of a trimethylaluminum/water ALD process, Chemical Vapor Deposition. 12 (2006) 275–279. https://doi.org/10.1002/cvde.200506433.

[31] G. Lehmpfuhl, A. Ichimiya, H. Nakahara, Interpretation of RHEED oscillations during MBE growth, Surface Science. 245 (1991) L159-162. https://doi.org/10.1016/0039-6028(91)90459-6.

[32] J.P. Podkaminer, J.J. Patzner, B.A. Davidson, C.B. Eom, Real-time and in situ monitoring of sputter deposition with RHEED for atomic layer controlled growth, APL Materials. 4 (2016) 086111. https://doi.org/10.1063/1.4961503.

[33] J.T. Gudmundsson, N. Brenning, D. Lundin, U. Helmersson, High power impulse magnetron sputtering discharge, Journal of Vacuum Science & Technology A: Vacuum, Surfaces, and Films. 30 (2012) 030801. https://doi.org/10.1116/1.3691832.